Seismic hybrid swarm precursory to a major lava dome collapse: 9-12 July 2003, Soufriere Hills Volcano, Montserrat

L. Ottemöller

British Geological Survey, Murchison House, West Mains Road, EH9 3LA, Edinburgh, UK

Abstract

A swarm of ≈ 9500 hybrid earthquakes preceded the 12-13 July 2003 dome collapse at Soufriere Hills Volcano, Montserrat. Most events had nearly identical waveforms and cross-correlation was applied to measure inter-event periods as well as phase arrival times to determine accurate relative location. Hypocenter depths were shallow (< 3 km), and relative locations were confined to a radius of < 150 m. This small source volume is consistent with the observed waveform similarity. Changes in inter-event periods and energy release, measured from the seismic records, showed that the volcano evolved through several energetic states, possibly linked to cyclic magma movement. Shorter inter-event periods were linked to higher energy release rates and possibly reflect increased pressurization during periods of low extrusion rates.

Key words: Montserrat, dome collapse, hybrid swarm, waveform correlation

1 Introduction

Following a dormancy of several centuries, the Soufriere Hills Volcano (SHV), Montserrat, in the northern part of the Lesser Antilles volcanic island arc, began erupting in July 1995 (Young et al., 1998; Kokelaar, 2002; Sparks and Young, 2002). The andesitic dome-building volcano remained active into early 1998 with a number of dome collapses, explosive activity and pyroclastic flows. A pause in the eruption occurred between March 1998 and November 1999, followed by renewed eruptive activity typified by periods of dome growth and collapses. Significant collapses occurred in March 2000 and July 2001. The lava dome reached maximum height and volume in July 2003, when the largest collapse of this eruption occurred (Herd et al., 2005). From about 12:00 UTC (all times hereafter UTC) on 12 July 2003 to 10:00 on 13 July, a volume of $\approx 210 \times 10^6$ m^3 collapsed from the SHV lava dome (Edmonds et al., 2004; Herd et al., 2005). This paper focuses on a swarm of hybrid seismic events that started on 9 July and preceded the dome collapse. The collapse in 2003 was followed by a pause in activity. Renewed extrusive activity started in August 2005 leading to a dome collapse in May 2006.

Seismic events at SHV are divided into four categories based on waveforms and frequency content (Miller et al., 1998; Neuberg et al., 1998): rockfalls and pyroclastic flows, long-period earthquakes (LPs) (Chouet, 1996b; Baptie et al., 2002), volcano-tectonic earthquakes (VTs) and hybrid events (Lahr et al.,

Email address: email: lot@bgs.ac.uk (L. Ottemöller).

1994). Hybrid events are a common and important type of seismic event at SHV (Miller et al., 1998), and are characterized by a high-frequency onset with mixed first motion polarities followed by a long-period coda. Although it was not possible to determine polarities for events in the 2003 swarm due to emergent P-waves, I follow the argument of Rowe et al. (2004) in terming the events "hybrids" without being able to confirm mixed first motion polarities. Some authors group hybrids and LPs together and refer to them as long-period earthquakes (e.g., Neuberg, 2000). Swarms of hybrid events have been observed at SHV prior to major volcanic events such as dome and edifice collapses (Miller et al., 1998; Calder et al., 2002; Voight et al., 1998), and their occurrence has been used as indication of potentially imminent hazard. The swarm starting on 9 July was recognized in this anticipatory sense by the Montserrat Volcano Observatory (MVO), where the author was the duty seismologist at the time.

Seismic events with similar waveforms and locations have been reported qualitatively at SHV (White et al., 1998). Rowe et al. (2004) applied cross-correlation techniques extensively to relocate 36 swarms of micro-earthquakes at SHV during 1995-1996. Within the swarms, waveforms were nearly identical, consistent with source volumes of about 1 km^3, as determined by multiple event location. Applying similar techniques, Green and Neuberg (2006) were able to identify families of similar events and relate these to tilt cycles for swarms at SHV in 1997. Stephens and Chouet (2001) showed how cross-correlation techniques can be used to quantify event swarms at Redoubt Volcano. The same events were analysed by Rowe (2000) who constrained locations to nearly a point source, consistent with previous results based on hypocenter statistics (Lahr et al., 1994). Waite et al. (2008) used cross-correlation techniques to quan-

tify similarities between long-period earthquakes at Mount St. Helens. They modeled the source as a combination of volumetric changes corresponding to resonance in a steam-filled crack and a vertical single force attributed to dome movement.

In this paper, I use cross-correlation techniques to retrospectively detect individual events during the July 2003 hybrid swarm from continuous data and to quantify similarity between the events. I also measured inter-event periods which together with a measure of event energy, provide a measure of the physical state of the volcanic system. The main objective of this article is the observation of inter-event periods and changes in energy release, which are discussed in the context of existing models. The systematic changes found may have implications for models of hybrid swarm generation. Finally, I use cross-correlation to determine accurate relative event locations, similar to Rowe et al. (2004). The availability of continuous data in 2003, meant that a more complete analysis of a single swarm could be done. The time scale of this study is 4 days, much shorter than the six months looked at by Rowe et al. (2004). The results obtained give important insights on the origin of the hybrid swarm and the SHV volcanic system. The results also demonstrate the potential usefulness of cross-correlation in real-time monitoring.

2 Data and Processing

Continuous seismic data were available from seven stations (Figure 1). The stations are operated by the MVO, except for station MBLY, which is operated by the University of Leeds. Data were available from stations MBGB, MBGH, MBLG and MBRY for the period 9-13 July 2003, while data from sta-

tion MBWH were only available from 10 July (16:00) onward. Station MBSS was operating, but its signal to noise ratio was too low and the data not used. Station MBLY had inaccurate timing for this period and could not be used for event locations. However, the data from MBLY was used in the cross-correlation analysis. The signal to noise ratio decreased with increasing distance from the source, but in general the swarm activity was well recorded. Hybrid events belonging to the swarm could not be detected during times when the swarm signal was overprinted by pyroclastic flow and rockfall activity. After 12:00 on 12 July, individual events merged into a continuous tremor (Figure 2) with the onset of nearly continuous pyroclastic flows (Herd et al., 2005) accompanying the early stage of the collapse. This study treats data from 00:00 July 9 to 12:00 July 12.

The continuous data were analyzed using a time domain cross-correlation technique that was implemented as part of this work to quantify similarities in the waveform signals and to measure inter-event periods, the time between two discrete events. Initial tests suggested that the majority of individual events had nearly identical waveforms. The waveforms from 20 identical events occurring on 12 July between 00:40 and 00:50 were stacked for each station to produce a set of representative master event waveforms (Figure 3) with increased signal to noise ratio. Events from this time period were chosen as the signal to noise ratio was relatively good. Stacked waveforms computed for other times were found to be well correlated with the set of master signals and gave results similar to the selected master signals. The master signals of fixed duration (Table 1) were band-pass filtered and then cross-correlated against the continuous data and events were detected when the cross-correlation was above a given threshold (Table 2). Consistent detection was achieved by in-

creasing the threshold from 9 July to 12 July, as event signal amplitudes increased over time resulting in a better signal to noise ratio. The analysis was automated to efficiently process the large number of events. Squared raw amplitudes were summed over a 10 s time window for individual events as a measure that is proportional to energy. Cumulative pseudo energy, as a measure that combines event frequency and amplitude, was calculated by adding these values over time. To show the changes in the cumulative energy, an averaged pseudo power was calculated by adding the energy from consecutive groups of 50 events (to show changes over 10-20 minute periods) and dividing by the time interval between the first and last events in the group. Waveform data were extracted for each detected event and used for subsequent single event processing. Figure 4 shows seismograms from a few sample events.

The extracted event data were processed further to determine accurate first arrival times. First, P-wave arrivals were picked manually for the set of stacked master signals. Then, the maximum of the cross-correlation function of the master signals with the event data was used to obtain absolute P-wave arrival times. Higher correlation threshold levels than in the detection processing were used here (Table 2). Detecting phase arrivals through cross-correlation techniques is judged more accurate and consistent than manual analysis (e.g., Got et al., 1986; Aster and Rowe, 2000; Rowe et al., 2002a,b, 2004; Schaff and Richards, 2004), particularly for small events. Events with five phase readings were then located using HYPOCENTER (Lienert and Havskov, 1995) for single event location and VELEST for joint hypocenter determination (JHD) (Kissling et al., 1994).

3 Inter-event periods, amplitudes and energy

Applying cross-correlation analysis to the continuous data, more than 7100 events exceeded the threshold criterion (Table 2), and were thereby detected and inter-event periods measured. This was consistent for all stations. The results were robust and correlation of master signals with noise only resulted in values less than half the threshold levels. Visual inspection and cluster analysis to identify events that differed significantly from the master waveforms failed, thus the > 7100 events can be considered a single family. Since the individual event durations were ≈ 12 s, inter-event periods of less than this time were not resolved. Attempts to detect smaller inter-event periods by deconvolving master from continuous waveforms failed due to the poor signal to noise ratio. Changes in inter-event period, signal amplitude, pseudo cumulative energy and pseudo power for events over the time period are given in Figure 5.

The inter-event periods display several branches (Figure 5). The lowest branch displays the highest density of points and gives the most likely period at a given time. Integration of the lowest branch results in a total of ≈ 9500 events throughout the whole time interval. This means the cross-correlation detection missed about 25% of the events. The additional branches are interpreted as "echo" patterns due to undetected events, either too small for detection or overlain by signals from other event types such as rockfalls. The "echo" patterns correspond to times when one or several events were missed. The scatter of points decreases from 9 to 12 July as waveform amplitudes increase, and fewer small events are missed.

The diagrams in Figure 5 show gradual changes rather than discontinuities

and reveal five distinct epochs characterized by changes in slope. Epochs 1, 3 and 5 are characterized by a gradual decrease in inter-event period from ≈ 30 to 15 s, with an increased rate of change toward the end of the epochs. Epochs 2 and 4 show a rise toward longer periods of 60 and 120 s respectively, which is then followed by a decrease to about 30 s. The increase and decrease are nearly symmetric, with a higher rate of change during epochs 2 and 4 than during the other epochs. Periods at the end of the epochs 2 and 4 are longer than at the respective beginnings and the rate of change starts decreasing when the period reaches about 30 s. The amplitudes systematically increase by a factor of 2 from epoch 1 to 5. The amplitude increase was largest at the end of epoch 1 and during epochs 2 and 4, while amplitudes remained nearly constant during epochs 3 and 5. The rate of increase in cumulative energy, seen as high pseudo power, was largest in epochs 3 and 5, reflecting the combination of larger amplitude and frequency of event occurrence. Figure 5 shows that correlation increased as amplitudes increased due to higher signal to noise ratio. But it also shows that correlation decreased as inter-event periods decreased at the end of epochs 3 and 5, caused by a decrease in signal to noise ratio related to the higher event frequency.

4 Hypocenter locations

Event locations were determined using P-wave arrival times determined by cross-correlation for a total of 661 events after 10 July 16:00 with phase readings on five stations (MBGB, MBGH, MBWH, MBLG and MBRY) (Figure 1). The absolute locations were poorly constrained, because of the limited number of phases for each event. The hypocenter locations were determined in two

steps. First, epicentre locations were fixed to the approximate conduit location (16.713°N/62.176°W, marked in Figure 1) to determine the best fitting absolute hypocenter depths and average velocity. This procedure was justifiable because previous studies had demonstrated that the hybrid events were closely tied to conduit processes and were generated near the conduit (Voight et al., 1999; Rowe et al., 2004). To avoid layer boundaries I used halfspace models with assumed P-wave velocities of 2.5, 3.0 and 3.5 km/s, similar to the velocity in the top layer of the model used at MVO. Mean RMS values for a range of fixed depths were computed using HYPOCENTER. The lowest RMS values were obtained for the 3 km/s velocity model and a hypocenter depth range of 0-3 km. The data did not allow for more accurate absolute depth determination. However, the velocity compares reasonably well with the 2.5 km/s determined for the top layer by Rowe et al. (2004).

Second, the same events were located using VELEST in joint hypocenter determination (JHD) mode with a fixed velocity of 3 km/s. JHD yields more precise relative locations, which allows for estimating the spread of hypocenter locations. The events were located within a horizontal radius of < 100 m over a depth range of about 300m (Figure 6). No change of hypocenter depth with time was observed. The source volume with a radius of < 150 m was similar to the results for single clusters in 1995-1996 (Rowe et al., 2004) and in 1997 (Green and Neuberg, 2006).

5 Interpretation and discussion

The main objective of this work was to quantify the properties and degree of similarity of hybrid events in the swarm precursory to the 12-13 July 2003

dome collapse. Cross-correlation analysis showed that at least 75% of the events belonged to a single family, with nearly identical waveforms. The remaining 25% probably also belong to this family as visual inspection did not find any significantly different waveforms. This contrasts with observations of a swarm in 1997, when several event families were observed (Green and Neuberg, 2006). The activity was also quite different before the dome collapse in May 2006, which was not preceded by a swarm of hybrid events (Luckett et al., in press). The high correlation recognized in the 2003 swarm mostly derives from the long period part of the signal, and is little affected by the higher frequency onset that contains information on the trigger source mechanism. This study demonstrates that cross-correlation techniques can be used to determine the total number of events in larger swarms of similar events, and to precisely measure inter-event periods. Tests with a standard phase picker showed that it can also do the job of detecting events. However, its performance is worse when noise levels are high and as it detects any signal changes less suited to measure inter-event periods of a specific event type. Using the cross-correlation technique, phase arrival times can be accurately and consistently measured for individual events. Hypocenter locations of 661 hybrid events calculated with VELEST in JHD mode using phase arrivals determined through cross-correlation fell within a single small source volume. This is consistent with the finding that all events occurring between July 9 and 12 were part of a single family. However, absolute locations were not well determined due to the limited number of stations and poor network geometry.

Several possible source mechanisms for hybrid events have been suggested based on the observation of signal similarities and their repetitive nature. Hybrid swarms of shallow origin at SHV were recognized within pressurization

cycles, with swarms occurring during inflation when extrusion rates are low and the system is pressurized (Voight et al., 1998, 1999; Sparks and Young, 2002). Denlinger and Hoblitt (1999) proposed a model of plug flow linked to cyclic changes in magma movement and volatile pressures. This model explains the cyclic changes at SHV for constant supply rates in the range of 2-10 m^3/s. The findings of Rowe et al. (2004) agree with hybrid event sources that involve rapid gas bubble formation or opening and closing of cracks. It has been suggested that only the involvement of fluids can provide a repetitive trigger mechanism for hybrid events where opening of cracks by excessive gas pressure is the trigger for these events (Chouet, 1996a; Neuberg et al., 1998; Waite et al., 2008). A brittle failure in the glass transition near the conduit wall was also suggested as a potential trigger (Neuberg et al., 2006). Voight and Elsworth (2000) demonstrated that gas pressurization can cause dome failure, which was supported by the study of Thomas et al. (2004). Once the energy is released, resonance within the conduit largely determines the shape of the later parts of the seismograms (Neuberg and O'Gorman, 2002; Jousset et al., 2003; Jousset and Neuberg, 2004). The fundamental frequency of resonance is determined by conduit geometry and contrast in elastic properties between the fluid magma and the solid rock.

The high waveform similarity for events in the July 2003 swarm confirmed the need for a repetitive trigger mechanism with a systematic frequency. Similarity of events requires a limited source volume, and location of the July 9-12 hybrid events indicate that the source volume was small. The changes in inter-event period and energy release reflect systematic changes in the conduit system through time. Observations for the July 2003 swarm showed that seismic energy release was highest when inter-event periods were short. These epochs

are possibly related to increased pressurization during periods of repose with low extrusion rates and inflation as seen in 1997 (Voight et al., 1998). Contrary, longer inter-event periods are possibly associated with rapid extrusion and reduced pressurization. While the measured inter-event periods indicated significant changes over time scales of several hours, they were remarkably stable over shorter times. This is consistent with observed oscillation periods of 4 to 30 hours in 1997 (Denlinger and Hoblitt, 1999). It should be noted that this model may not be valid for other volcanoes. For example, at Mount St. Helens in 2005, changes in inter-event periods appear to be related to dome activity (Moran et al., 2005b), but may not be linked to changes in extrusion rates (Moran et al., 2005a).

Occurrence of the July 2003 hybrid swarm prior to a major dome collapse, raises the question whether the events were the result of increased pressurization that weakened the volcanic edifice and eventually triggered or caused dome failure. While this is possible, giving a conclusive answer is beyond the scope of this paper. Alternatively, the onset of heavy rain during the latter phase may have contributed to destabilizing the dome (Herd et al., 2005). Comparison with deformation data from either tiltmeter or short term continuous GPS data would provide further evidence, but in 2003 no tiltmeter was operational at SHV and GPS data were processed as daily averages.

6 Conclusions

The hybrid swarm preceding the 12-13 July 2003 dome collapse consisted of ≈ 9500 events. Nearly identical waveforms were found for $\approx 75\%$ of the events implying a repetitive and stationary source. Cross-correlation techniques were

applied to consistently and accurately measure inter-event periods and phase arrival times. The events originated from a source volume with a radius of $<$ 150 m without observing any hypocenter migration over time. The changes in inter-event period and energy release are possibly related to the dynamics of the conduit system, controlled by supply rate, extrusion rate and pressurization (Melnik and Sparks, 2002). Epochs with increased energy release and short inter-event periods possibly correlate with increased pressurization linked to a low extrusion rate and inflation. As predicted by cyclic pressurization models, these epochs are followed by epochs with longer inter-event periods and lower energy release, possibly linked to increased extrusion rates and deflation. The increased pressurization causing the hybrid swarm may have contributed to destabilizing the dome. The occurrence of hybrid swarms at SHV, can therefore be a precursor of catastrophic failure. While the interpretation given here is somewhat speculative, existing models for the generation of hybrid swarms at SHV need to be tested against the observations of regular inter-event periods that undergo systematic changes through time. Measuring inter-event periods and energy release characterizes the state of the conduit system and can be useful in real-time monitoring.

7 Acknowledgments

This work has greatly benefited from discussions with G Ryan, R Luckett and B Baptie. The paper has significantly benefited from comments on an earlier version of the manuscript by C A Rowe and B Voight. Review comments by P Jousset and an anonymous reviewer helped to improve the manuscript. Data were provided by the MVO and the MULTIMO project. This paper is

published with permission of the Executive Director of the British Geological Survey (NERC).

References

Aster, R. C., Rowe, C. A., 2000. Automatic phase pick refinement and similar event association in large seismic datasets. In: Thurber, C., Rabinowitz, N. (Eds.), Advances in seismic event location. Kluwer, pp. 231–263.

Baptie, B., Luckett, R., Neuberg, J., 2002. Variability of seismic tremor episodes at Soufriere Hills Volcano. Geological Society, London, Memoirs 21, 611–620.

Calder, E. S., Luckett, R., Sparks, R. S. J., Voight, B., 2002. Mechanisms of lava dome instability and generation of rockfalls and pyroclastic flows at Soufriere Hills Volcano, Montserrat. Geological Society, London, Memoirs 21, 173–190.

Chouet, B., 1996a. New methods and future trends in seismological volcano monitoring. In: R. Scarpa and R. Tilling (Ed.), Monitoring and mitigation of volcano hazards. Springer-Verlag, New York, pp. 23–97.

Chouet, B. A., 1996b. Long-period volcano seismicity: Its source and use in eruption forecasting. Nature 380, 309–316.

Denlinger, R., Hoblitt, R., 1999. Cyclic eruptive behavior of silicic volcanoes. Geology 27, 459–462.

Edmonds, M., Herd, R. A., Strutt, M., Sanchez, J., Dunkley, P., Ryan, G., Bass, V., Mann, C., 2004. Dome collapse and explosive activity, 12-15 July 2003. MVO Special Report 10.

Got, J. L., Fremont, J. J., Frechet, J., 1986. Kilauea and Mount Saint Helens volcanic earthquake doublets. Reun. Annu. Sci. Terre 11, 82.

Green, D., Neuberg, J., 2006. Waveform classification of volcanic low-frequency swarms and its implication. J. Volcan. Geotherm. Res.Doi:10.1016/j.jvolgeores.2005.08.008.

Herd, R. A., Edmonds, M., Bass, V. A., 2005. Catastrophic lava dome failure at Soufriere Hills Volcano, Montserrat, 12-13 July 2003. J. Volcan. Geotherm. Res. 148, 234–252.

Jousset, P., Neuberg, J., 2004. Modelling low-frequency volcanic earthquakes in a viscoelastic medium with topography. Geophys. J. Int. 159, 776–802.

Jousset, P., Neuberg, J., Sturton, S., 2003. Modelling the time-dependent frequency content of low-frequency volcanic earthquakes. J. Volcan. Geotherm. Res. 128, 201–223.

Kissling, E., Ellsworth, W. L., Eberhart-Phillips, D., Kradolfer, U., 1994. Initial reference model in local earthquake tomography. J. Geophys. Res. 99, 19635–19646.

Kokelaar, B. P., 2002. Setting, chronology and consequences of the eruption of Soufriere Hills Volcano, Montserrat (1995-1999). Geological Society, London, Memoirs 21, 1–43.

Lahr, J. C., Chouet, B. A., Stephens, C. D., Power, J. A., 1994. Earthquake classification, location, and error analysis in a volcanic environment: implications for the magmatic system of the 1989-1990 eruptions of Redoubt Volcano, Alaska. J. Volcan. Geotherm. Res. 62, 137–151.

Lienert, B. R. E., Havskov, J., 1995. A computer program for locating earthquakes both locally and globally. Seis. Res. Lett. 66, 26–36.

Luckett, R., Loughlin, S., Angelis, S. D., Ryan, G., in press. Volcanic seismicity at Montserrat, a comparison between the 2005 dome growth episode and earlier dome growth. J. Volcan. Geotherm. Res.

Melnik, O., Sparks, R. S. J., 2002. Dynamics of magma and lava extrusion at

Soufriere Hills Volcano, Montserrat. Geological Society, London, Memoirs 21, 153–171.

Miller, A. D., Stewart, R. C., White, R. A., Luckett, R., Baptie, B. J., Aspinall, W. P., Latchman, J. L., Lynch, L. L., Voight, B., 1998. Seismicity associated with dome growth and collapse at the Soufriere Hills Volcano, Montserrat. Geophys. Res. Lett. 25, 1995–1997.

Moran, S. C., Malone, S. D., Qamar, A. I., Thelen, W., Waite, G., Horton, S., Lahusen, R. G., Major, J. J., 2005a. Overview of seismicity associated with the 2004-2005 eruption of Mount St. Helens, Abstract V52B-02. EOS Trans. AGU 86(52).

Moran, S. C., Qamar, A. I., Buurman, H. M., 2005b. Automated Earthquake Detection During the 2004-2005 Eruption of Mount St. Helens, Abstract V53D-1600. EOS Trans. AGU 86(52).

Neuberg, J., 2000. Characteristics and causes of shallow seismicity in andesite volcanoes. Philosophical Transactions of the Royal Society of London 358, 1533–1546.

Neuberg, J., Baptie, B., Luckett, R., Stewart, R., 1998. Results from the broad-band seismic network on Montserrat. Geophys. Res. Lett. 25, 3661–3664.

Neuberg, J., O'Gorman, C., 2002. A model of the seismic wavefield in gas-charged magma: application to Soufriere Hill Volcano, Montserrat. Geological Society, London, Memoirs 21, 603–609.

Neuberg, J., Tuffen, H., Collier, L., Green, D., Powell, T., 2006. The trigger mechanism of low-frequency earthquakes on Montserrat. J. Volcan. Geotherm. Res.Doi:10.1016/j.jvolgeores.2005.08.008.

Rowe, C. A., 2000. Correlation-based phase pick correction and similar earthquake identification in large seismic waveform catalogues. New Mexico Institute of Mining and Technology, PhD thesis.

373 Rowe, C. A., Aster, R. C., Borchers, B., Young, C. J., 2002a. An automatic,
374 adaptive algorithm for refining phase picks in large seismic data sets. Bull.
375 Seismol. Soc. Am. 92, 1660–1674.
376 Rowe, C. A., Aster, R. C., Phillips, W. S., Jones, R. H., Borchers, B., Fehler,
377 M. C., 2002b. Using automated, high-precision repicking to improve delin-
378 eation of microseismic structures at the Soultz geothermal reservoir. Pure
379 Appl. Geophys. 159, 563–596.
380 Rowe, C. A., Thurber, C. H., White, R. A., 2004. Dome growth behaviour at
381 Soufriere Hills Volcano, Montserrat revealed by relocation of volcanic event
382 swarms, 1995-1996. J. Volcan. Geotherm. Res. 134, 199–221.
383 Schaff, D. P., Richards, P. G., 2004. Repeating seismic events in China. Science
384 303, 1176–1178.
385 Sparks, R. S. J., Young, S. R., 2002. The eruption of Soufriere Hills Volcano,
386 Montserrat (1995-1999): overview of scientific results. Geological Society,
387 London, Memoirs 21, 45–69.
388 Stephens, C. D., Chouet, B. A., 2001. Evolution of the December 14, 1989
389 precursory long-period swarm at Redoubt Volcano, Alaska. J. Volcan.
390 Geotherm. Res. 109, 133–148.
391 Thomas, M. E., Petford, N., Bromhead, E. N., 2004. The effect of internal
392 gas pressurization on volcanic edifice stability: evolution towards a critical
393 state. Terra Nova 16, 312–317.
394 Voight, B., Elsworth, D., 2000. Instability and collapse of hazardous gas-
395 pressurized lava domes. Geophys. Res. Lett. 27, 1–4.
396 Voight, B., Hoblitt, R. P., Clarke, A. B., Lockhart, A. B., Miller, A. D., Lynch,
397 L. L., McMahon, J., 1998. Remarkable cyclic deformation monitored in real
398 time on Montserrat and its use in eruption forecasting. Geophys. Res. Lett.
399 25, 3405–3408.

Voight, B., Sparks, R. S. J., Miller, A. D., 1999. Magma flow instability and cyclic activity at Soufriere Hills Volcano, Montserrat, British West Indies. Science 283, 1138–1142.

Waite, G. P., Chouet, B. A., Dawson, P. B., 2008. Eruption dynamics at Mount St. Helens imaged from inversion of broadband waveforms: interaction of the shallow magmatic and hydrothermal system. J. Geophys. Res. 113, B02305.

White, R. A., Miller, A. D., Lynch, L., Power, J., 1998. Observations of hybrid seismic events at Soufriere Hills volcano, Montserrat: July 1995 to September 1996. Geophys. Res. Lett. 25, 3657–3660.

Young, S. R., Sparks, R. S. J., Aspinall, W. P., Lynch, L. L., Miller, A. D., Robertson, R. E. A., Shepherd, J., 1998. Overview of the eruption of Soufriere Hills Volcano, Montserrat, July 18, 1995, to December 1997. Geophys. Res. Lett. 25, 3389–3392.

Table 1

Processing parameters used to compute cross-correlation and minimum correlation coefficients for 9-12 July.

Station Code	Component Code	Duration (s)	Band-pass filter (Hz)
MBLY	BHZ	7.	1.-5.
MBRY	BHZ	12.	1.-5.
MBGH	BHZ	12.	1.-5.
MBGB	BHZ	12.	2.-5.
MBLG	SHZ	12.	1.-5.
MBWH	SHZ	12.	1.-5.

Table 2

Minimum correlation coefficients required for event detection. It is the same for all stations.

Day July	Correlation threshold continuous data	Correlation threshold event data
09	0.60	0.70
10	0.62	0.70
11	0.64	0.70
12	0.66	0.70

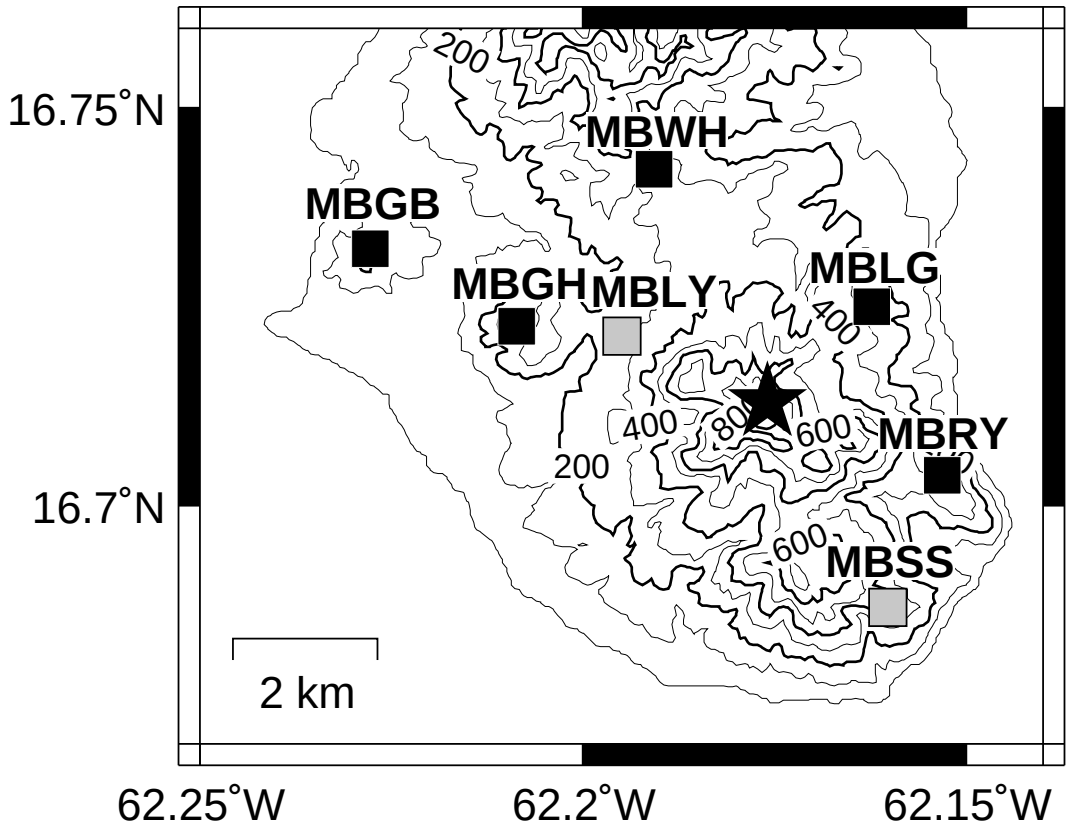

Fig. 1. Seismic stations used for event location are shown as black squares. All stations except MBLY (University of Leeds) are operated by the MVO. Stations MBGB, MBGH, MBLY and MBRY are equipped with broadband seismographs, while stations MBLG, MBWH and MBSS use short period instruments. Station MBSS was too noisy to be used. Data from MBWH was available only after July 10. The approximate conduit location is marked by the star.

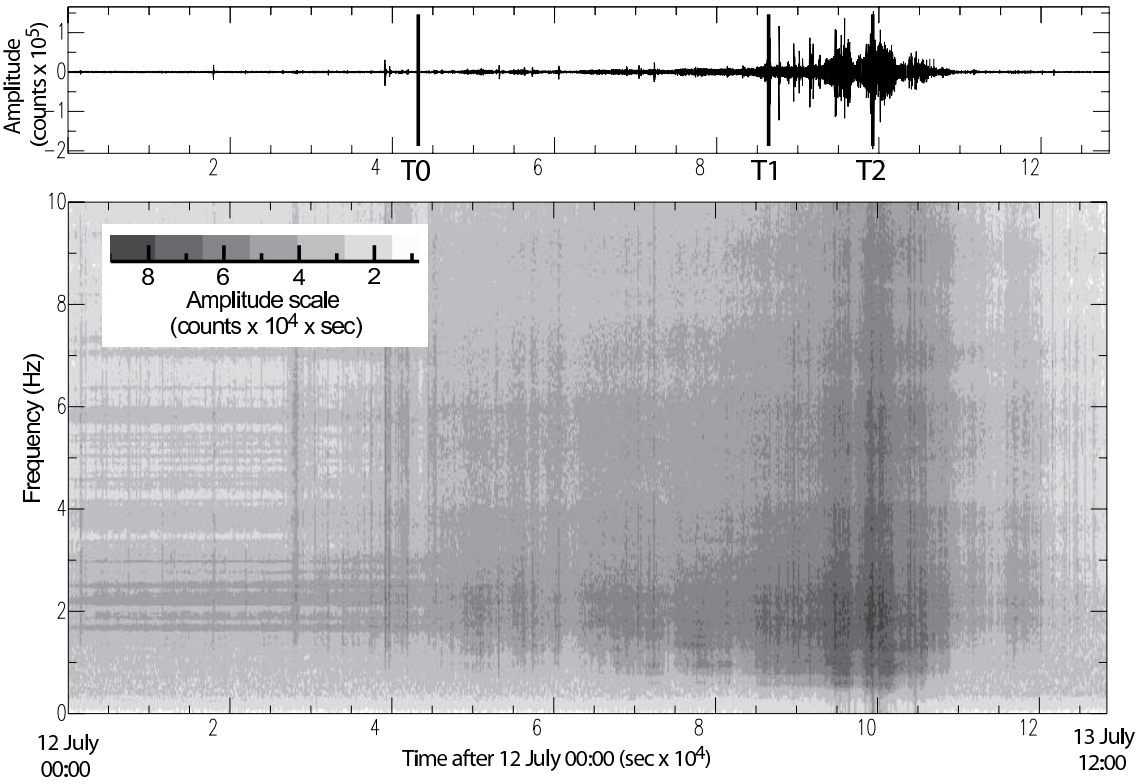

Fig. 2. Seismogram (top) and spectrogram (bottom) for station MBWH for period 12 July 00:00 to 13 July 12:00. Time markers are: T0 = 12 July 12:00 (onset of tremor), T1 = 13 July 00:00 (onset of period with highest seismic energy release) and T2 = 13 July 03:35 (time of maximum seismic signal energy). The hybrid swarm with distinctive events is seen only until T0 as lines around 2 Hz in the spectrogram.

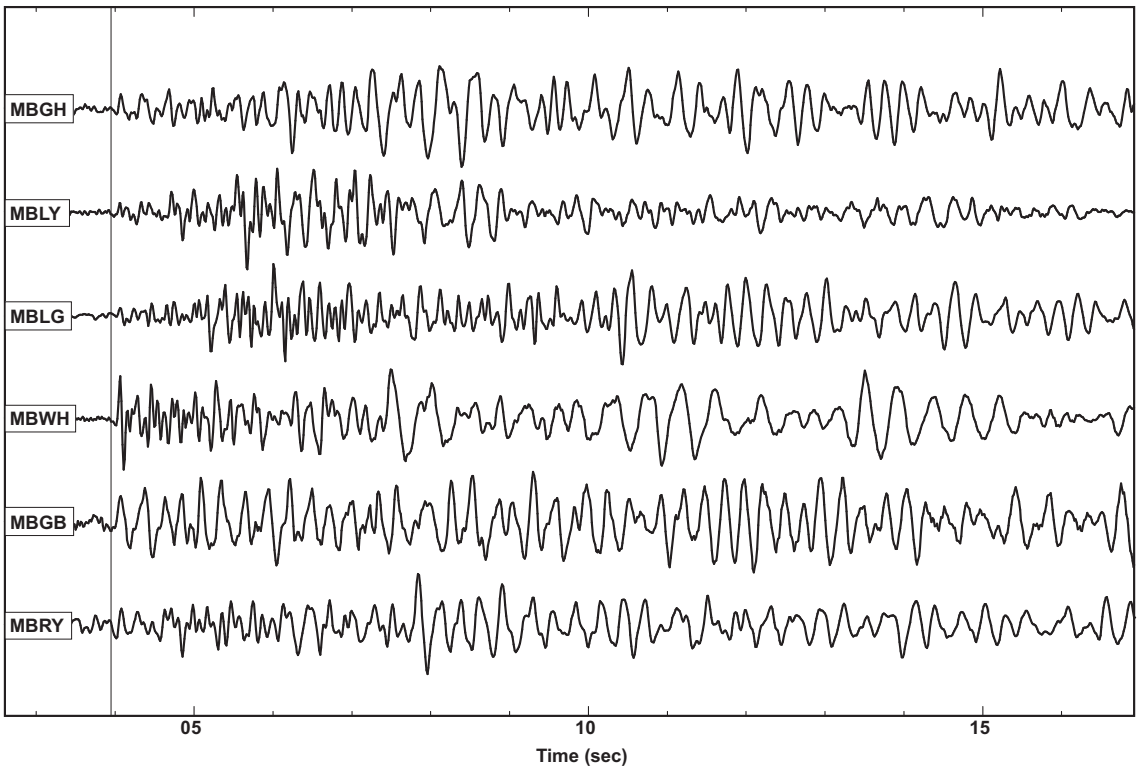

Fig. 3. Stacked signals used as master event from 20 individual events between 00:40 and 00:50 on 12 July. The data in this plot are high-pass filtered with a cut-off frequency of 2 Hz. The vertical line indicates the P-wave arrival.

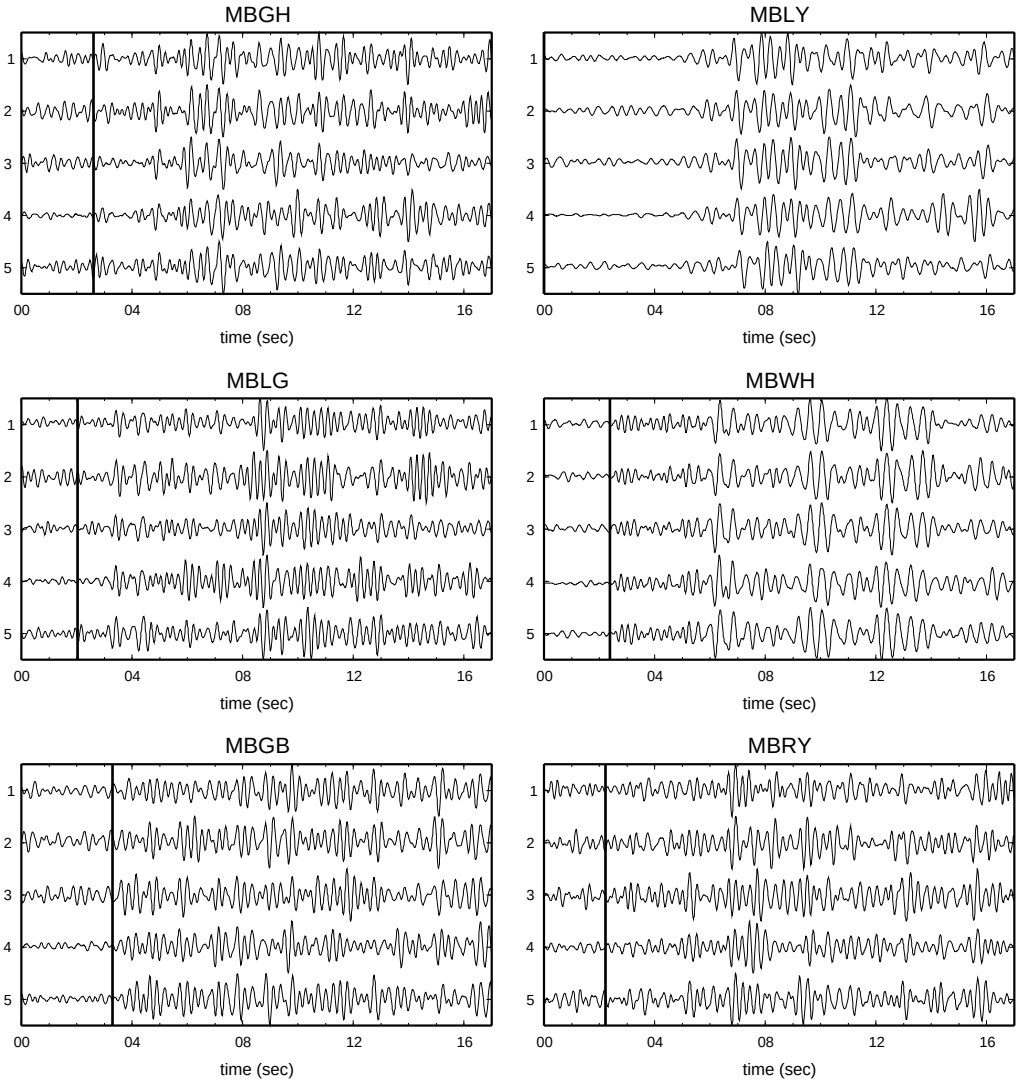

Fig. 4. Seismograms from five randomly selected events are plotted for six stations. The reference time (0 s) is the same for all stations and the expected arrival times are marked by a vertical line. The date and time of the events as indexed on the y-axis are: 1) 10 July 17:57, 2) 11 July 00:00, 3) 11 July 10:38, 4) 11 July 15:29 and 5) 12 July 00:06. The data are filtered with a pass-band of 2-5Hz. Note that station MBLY is not used for locating the events and only shown to demonstrate that the waveforms are correlated.

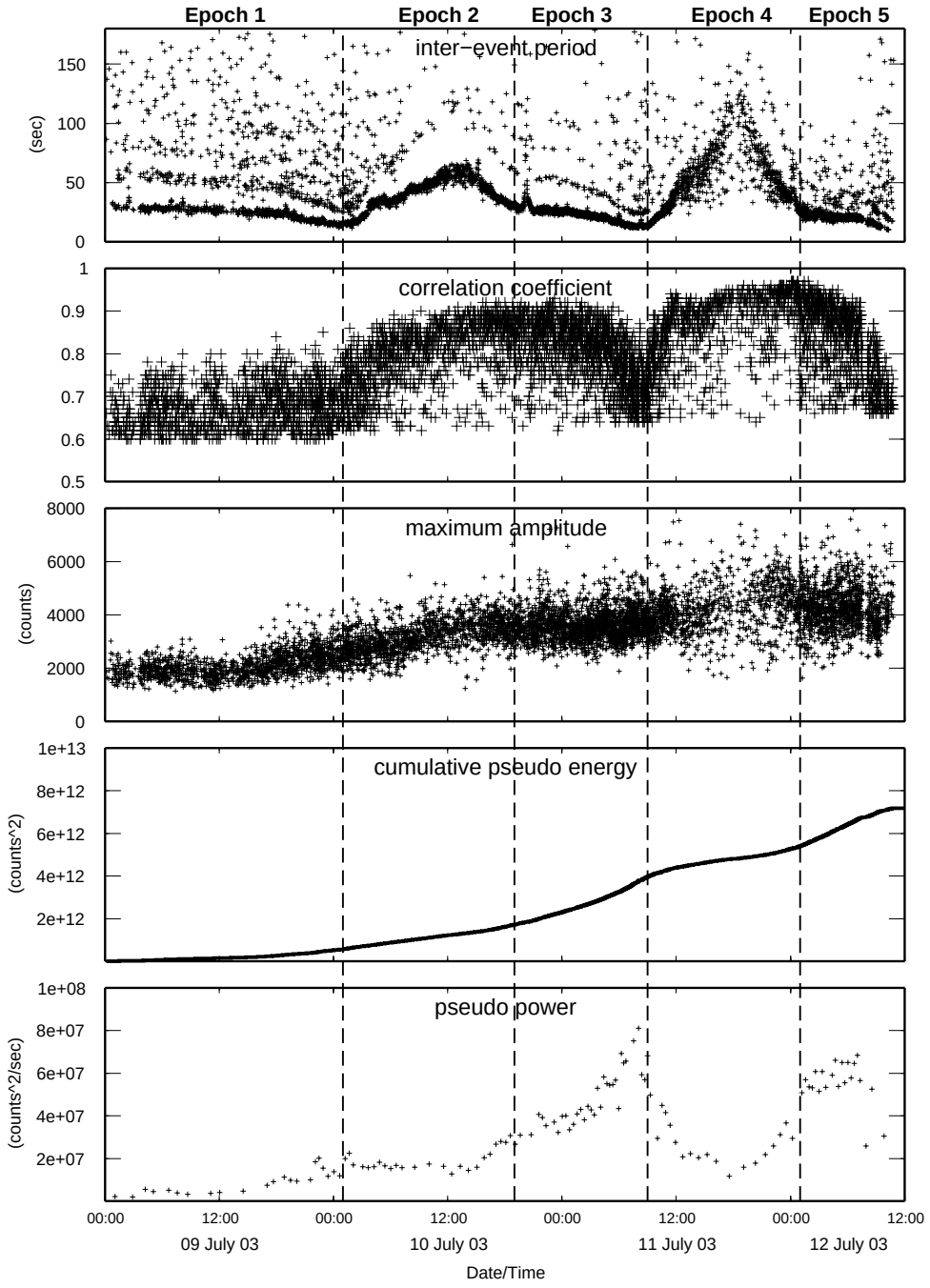

Fig. 5. Inter-event period, correlation coefficient, maximum amplitude, pseudo cumulative energy and pseudo power determined for station MBLG between 00:00 July 9 and 12:00 July 12. Based on these results, the time interval can be divided into five epochs indicated by vertical lines, see main text.

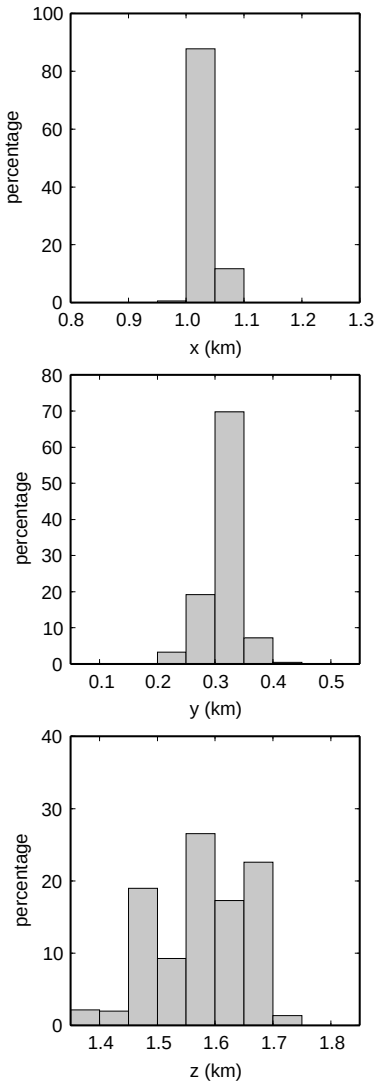

Fig. 6. Histograms showing distribution of hypocenter spread determined by joint hypocenter determination for the 661 events with five onset times. The coordinates only give the scale for relative locations, but are not correct in absolute terms. The origin of the cartesian coordinate system is 16.714N/62.176W.